Received 19 April 2024; revised 9 September 2024; accepted 13 September 2024. Date of publication 23 September 2024; date of current version 30 January 2025.

Digital Object Identifier 10.1109/OJAP.2024.3465652

Frequency Diverse Array for Signal Geofencing in Wireless Communications: Does it Work?

SIMONE DEL PRETE (Member, IEEE), MARINA BARBIROLI, AND FRANCO FUSCHINI

Department of Electrical, Electronic and Information Engineering "G. Marconi", University of Bologna, 40126 Bologna, Italy

CORRESPONDING AUTHOR: F. FUSCHINI (e-mail: franco.fuschini@unibo.it)

ABSTRACT Frequency Diverse Array is an advanced antenna technology for clustering received power spatial distribution in specific areas, which has shown significant potential in many applications, including radar or wireless power transfer. In wireless communications, signal geofencing might be beneficial in increasing communication secrecy or reduce interference issues, but system communications through frequency diverse arrays require careful consideration about several design parameters. In this paper, a detailed analysis of the sensitivity of the geofencing effectiveness to the main array parameters is carried out. The analysis covers many aspects of the design, including the selection of the geometrical layout and the number of elements of the array, the frequency increase policy and the frequency offset across the elements and their spacing. The study also discusses the trade-offs between different design choices and provides insights into the performance in terms of focus efficiency and size of the focus area. Results show that bidimensional layouts, e.g., circular or planar, often represent effective solutions, whereas the linear arrangement can be a viable option only in case the frequencies are spread across the elements in a random-like fashion. Frequencies are usually increased according to either a logarithmic or a linear policy. The linear solution in general yields lower performance, but also lower complexity. Frequency offset, number of elements and their spacing represent further project parameters. Finally, a preliminary assessment of the multipath effect on the focus task shows that the performance of frequency diverse arrays can be affected by complex propagation conditions and deserve further investigations.

INDEX TERMS Frequency diverse array, geofencing, physical layer security, electromagnetic propagation.

I. INTRODUCTION

A TRANSMITTING antenna array is referred to as frequency diverse (FDA) if the different radiating elements are supplied by feeding signals at different frequencies [1], [2]. Frequency diversity enables "power spatial focusing", i.e., the possibility for the radiated field to peak around some target point(s), i.e., at some specific distance in some specific direction and at some instants of time [1], [2], [3], [4]. In principle, this corresponds to a better control of the transmitted power spatial distribution compared to standard phased array, which can only enforce "beam angular steering", i.e., boost the electromagnetic radiation in some privileged, spatial direction(s). Nevertheless, the array solution can increase the field intensity of a single radiating element by a factor always equal to the number of radiating elements at most, regardless of whether the array is frequency diverse or not. Therefore, the real advantage brought by FDAs compared to standard arrays is not a further boost of intensity in the target point, but rather a lower intensity outside the target spot. In this respect, "signal geofencing" or "power spatial filtering" might be effective alternatives to "power spatial focusing" to describe the major goal of FDAs.

Although FDA techniques have been mainly envisaged for radar and navigation [1], [2], [5], [6], [7], [8], they have been also recently proposed for wireless power transfer [9], [10]. In the framework of wireless communication systems, signal geofencing can be potentially beneficial in a twofold way, i.e., to manage interference issues and to enforce communications secrecy [11], [12], [13]. As a matter of fact, limiting the intensity of the transmitted signal outside a spot placed on the target receiver also reduces the interference brought

to other users. At the same time, providing a satisfactory signal-to-noise ratio only at the target receiver can also limit the access of possible eavesdroppers to the information content exchanged by two legitimate users. Of course, FDA techniques for both secrecy and interference control require information about the users' position, i.e., they belong to the class of *location aware* wireless applications [14], [15]. Wireless positioning has been gaining increasing interest over the years, to the extent that it is now a common feature of many user equipment. Indoor localization performance might be still imprecise in some cases - mostly because of obstruction and multipath impairments - but technical progress (e.g., based on Machine Learning) is expected to further improve indoor positioning accuracy [16], [17]. In order that the potential advantages offered by FDAs to wireless communications become real opportunities, the size and the shape of the geofencing area has to be carefully set. If it is exceedingly large, mitigation of both interference and eavesdropping threat might be naively impaired; conversely, if it is uselessly small, its placing on the target receiver could be difficult, unless very precise information about its position is available. Furthermore, it is worth pointing out that signal geofencing is unavoidably time-dependent, i.e., it can be enforced at the target point at some time intervals, but not forever [3], [11], unless the phase of the feeding signals can be adaptively tuned. Although often neglected in previous studies [13], [18], this represents a crucial aspect that can cast a shadow on the real convenience of FDA for effective signal geofencing. Nevertheless, FDAs can be arranged in order that spatial focusing is periodic over time, thus supplying authorized users with multiple time slots for reliable communications, provided that synchronization is also supported. Moreover, transmission can be interrupted as soon as the array beam spot is no longer fairly placed on the target receiver, thus anyway preventing any eavesdropper from the access to private data [19].

Most of the existing studies on FDA for wireless communications mainly deal with effective schemes and algorithms to arrange the signals feeding the radiating elements to limit interference and/or pursue communication privacy, whereas the antenna layout is always and simply limited to the uniform linear case [3], [13], [15], [18], [20], [21]. By contrast, a thorough investigation on the impact of the main antenna array parameters (like the number of elements, their spatial deployment and spacing, the arrangement of the frequencies across them) on the geofencing effectiveness is carried out in this work. Moreover, some major relationships so far not fully highlighted between signal geofencing in the time and in the spatial domain are also addressed. The outcomes of the following investigation can provide useful design guidelines and highlight practical limitations for geofencing applications.

A comparative summary of the main research activities carried out on FDA is reported in Table 1.

The paper is organized as follows: formal description of FDA principles under free space propagation conditions are included in Section II, whereas signal geofencing in the space and in the time domain is targeted in Section III. Geofencing sensitivity to FDA parameters is described in Section IV, and preliminary assessment of the performance of FDA in a multipath environment is finally addressed in Section V. Section VI briefly includes some general considerations on multi-user FDA communications, whereas some conclusions are finally drawn in Section VII.

II. FREE SPACE RADIATION FROM FDAS

Under the usual narrowband approximation, the signal feeding the m-th element of a transmitting FDA made by M elements is expressed as:

$$\begin{aligned} s_m(t) &= S_m \cos(2\pi f_m t + \delta_m) \\ &= S_m \cos\left[2\pi (f_0 + \Delta f_m)t + \delta_m\right] \end{aligned} \tag{1}$$

where Δf_m is the frequency increase at the m-th element ($m = 0, 1, \ldots, M-1$) with respect to the single, reference element (herein conventionally labeled with m=0). Frequencies are usually deployed over the array according to either a linear or a logarithmic policy [1], i.e.:

$$\Delta f_m = m\Delta f \tag{2}$$

$$\Delta f_m = \log(m+1)\Delta f \tag{3}$$

being Δf a fixed frequency offset. Although the different frequencies are usually assigned to the array elements according to a simple, incremental scheme (i.e., the increase Δf_m applied to the m-th element), solutions based on a random distribution of the frequencies across the array (i.e., the increase Δf_m applied to the m'-th element, with m in general different from m') have been also investigated [22] and are also further considered in this work.

The free space, far-field radiated by an FDA can be expressed according to the classical formulation generally adopted for standard array, i.e., as the product between the field generated by the single, reference element (E_0) and a proper array factor (AF). With respect to standard arrays, the array factor of FDAs depends not only on angle(s) but also on both range and time. This is shown in the following subsections, where the far-field computation is carried out for three different spatial arrangements of the radiating elements. In agreement with previous studies, the analysis is limited to free space propagation conditions and to a 2D spatial domain for the sake of simplicity.

A. LINEAR DEPLOYMENT

Let's consider M isotropic sources linearly deployed, as sketched in Fig. 1. The AF value in a generic point (R, θ) of the XY plane can be expressed as:

$$\begin{aligned} AF(R,\theta,t) = \sum_{m=0}^{M-1} & e^{j\delta_m} e^{j\frac{2\pi f_0 md\sin\theta}{c}} \\ & e^{-j\frac{2\pi\Delta f_m(R-md\sin\theta)}{c}} e^{j2\pi\Delta f_m t} \end{aligned} \tag{4}$$

TABLE 1. Summary of related works.

Reference	FDA layout	Frequency settings	Propagation conditions	Performance marker	Application field
[1]	Linear	Linear, logarithmic	Free space	Array Factor	Radar
[2]	Linear	Linear	Free space	Array Factor	Radar
[3]	Linear	Linear increase	Free space	Array Factor, time analysis	Communication, WPT
[5]	Linear	Logarithmic	Free space	Array Factor	Radar
[7]	Linear	Linear	Free space	Array Factor	Radar and navigation
[9]	Linear	Multi-sine	Free space	Array Factor	WPT
[10]	Linear	Logarithmic	Free space	Array Factor	WPT
[13]	Linear	Linear increase	Free space	Array factor	Secure communications, Directional modulation
[15]	Linear	Optimized for Secrecy Rate Maximization	Free space	Secrecy rate	Secure communication
[19]	Planar	Time controlled, linear	Simulated free space, measured indoor	Array Factor, Received power	WPT
[20]	Linear	Optimized for Fixed Region Beamforming using Frequency Diverse Subarray	Free space	Array factor, secrecy rate	Secure communications
This work	Linear, Planar, Circular	Linear, Logarithmic	Free space, two rays model	Array Factor, Time Analysis, Focus Area, Focus Efficiency	Secure communications, Interference management

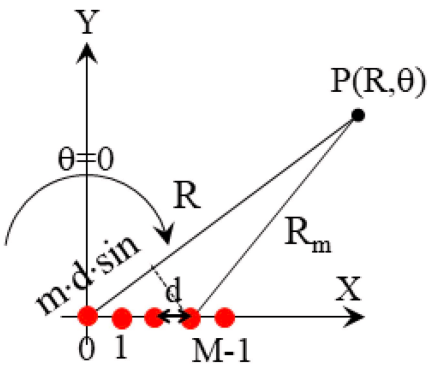

FIGURE 1. Deployment of a linear FDA.

where f_0 is the frequency feeding the reference element and δ_m the phase of the signal feeding the $m-$th element. Further details are included in the Appendix A.

If the goal of the FDA is to make the field peaking in a target point, $P_t(R_t, \theta_t)$ the phase δ_m of the signal feeding the $m-th$ element must be set as follows:

$$\delta_m^{peak} = \beta_0 R_t - \frac{2\pi m f_0 d \sin\theta_t}{c} + 2\pi \frac{\Delta f_m}{c}[R_t - (m)\ d \sin\theta_t] - 2\pi \Delta f_m t \quad (5)$$

According to eq. (5) the phase coefficients should be continuously tuned over time to keep the peak of the field on P_t. In case of static geofencing, where the target point keeps still, the phase values must linearly change over time, thus corresponding to a saw-tooth phase modulation profile. Conversely, the phase-time relationship turns out much harder in case P_t is moving (i.e., in mobile wireless communications), to the extent that geofencing may result simply impossible unless accurate and up-to-date information on the target point position can be provided to the transmitting FDA. This issue is mitigated in case mobility occurs at somehow constant speed and along the same, specific track, as for instance in railways [23]. In order to reduce the complexity of the phase tuning procedure, the peak condition is often limited to some instant t_0 (usually set as $t_0 = 0$ for the sake of simplicity [1]), i.e.:

$$\delta_m^{peak} = \beta_0 R_t - \frac{2\pi m f_0 d \sin\theta_t}{c} + 2\pi \frac{\Delta f_m}{c}[R_t - md \sin\theta_t] - 2\pi \Delta f_m t_0 \quad (6)$$

In order that two legitimate users can effectively exchange some information through the FDA communications, the field should steadily peak in the target receiving location P_t for a time (much) greater than the symbol length. Of course, this requirement is automatically met if the phases can be set according to eq. (5), as the field peak will be then steadily placed on P_t. By contrast, if the condition in eq. (6) is instead enforced, the array factor is going to change over time at a rate related to Δf_m (eq. (4)), and the following relation

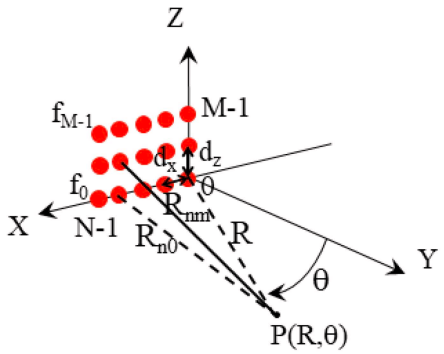

FIGURE 2. Planar deployment of an FDA.

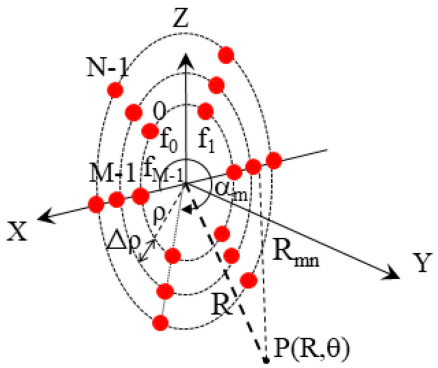

FIGURE 3. Multiple rings circular deployment of an FDA.

should be therefore fulfilled (also in agreement with [1]):

$$\Delta f_m \ll B \ll f_0, \quad \forall m \tag{7}$$

Moreover, in case a large amount of data must be exchanged, the peak should periodically turn up at the target receiving locations in order to provide multiple time slots for communication. This aspect will be further discussed in the following.

In the framework of resorting to FDA to improve the privacy of communications, transmission of artificial noise to knock down the signal-to-noise ratio of possible eavesdropper has been also proposed [24], [25]. Since artificial noise of course should not be delivered to the legitimate receiver, the array factor should now have a notch in P_t. The phase δ_m of the signal feeding the $m-th$ element must be then set as:

$$\delta_m^{notch} = \delta_m^{peak}, \delta_{m+1}^{notch} = \delta_{m+1}^{peak} + \pi$$
$$m = 1, 3, 5.., M-1 \tag{8}$$

In case large array size can be afforded, part of the array could be devoted to focus the signal on the target receiver, whereas the remaining elements could be employed to spread artificial noise all around.

B. PLANAR DEPLOYMENT

With reference to the planar deployment shown in Fig. 2 let N and M be the number of elements along the X and the Z axis, respectively, whereas d_x and d_z are the corresponding spacings. The feeding frequency does not change along X axis, but only along Z axis. The distance between the (n, m) element on the grid and the point P can be clearly expressed as:

$$R_{nm} = \sqrt{R_{n0}^2 + (m \cdot d_z)^2} \tag{9}$$

Under far-field conditions, the distance between the element (n,0) and P can be still computed as in eq. (A.3) by simply replacing m with n and d with d_x. Then:

$$R_{nm} \approx \sqrt{(R - n d_x \sin\theta)^2 + (m \cdot d_z)^2} \tag{10}$$

The array factor can be therefore expressed as:

$$AF(R, \theta, t) = \sum_{n=0}^{N-1} \sum_{m=0}^{M-1} e^{j\delta_{nm}} e^{j\frac{2\pi f_0}{c}(R_{nm}-R)} e^{-j\frac{2\pi \Delta f_m R_{nm}}{c}} e^{j2\pi \Delta f_m t} \tag{11}$$

The phase values required to set the peak in P_t at time instant t_0 can be then written as:

$$\delta_{nm} = \beta_0 R_{nm} + \frac{2\pi \Delta f_m R_{nm}}{c} - 2\pi \Delta f_m t_0 \tag{12}$$

C. CIRCULAR DEPLOYMENT

In addition to the linear and the planar deployment, the circular layout reported in Fig. 3 is also here considered. Frequency diversity is applied across the M elements over each circle, whereas the N elements on the same spoke share the same frequency [26]. Also, the elements are uniformly spaced in both the radial and the angular direction. The far-field approximation for the element-to-point P distance and the corresponding expression of the array factor are reported in eq. (13) and eq. (14), respectively.

$$R_m \approx R - (\rho + n\Delta\rho)\sin\theta\cos\alpha_m \tag{13}$$

$$AF(R, \theta, t) = \sum_{n=0}^{N-1} \sum_{m=0}^{M-1} e^{j\delta_{mn}} e^{j\frac{2\pi f_0}{c}(\rho+n\Delta\rho)\sin\theta\cos\alpha_m} e^{-j\frac{2\pi \Delta f_m}{c}(R-(\rho+n\Delta\rho)\sin\theta\cos\alpha_m))} e^{j2\pi \Delta f_m t}. \tag{14}$$

Eq. (14) easily provides the phase shift δ_{mn} required to set up the field peak in P_t at time instant t_0:

$$\delta_{mn} = \beta_0 R_t + \frac{2\pi \Delta f_m}{c}[R_t - (\rho + n\Delta\rho)\sin\theta_t\cos\alpha_m] - \frac{2\pi f_0}{c}(\rho + n\Delta\rho)\sin\theta_t\cos\alpha_m - 2\pi \Delta f_m t_0 \tag{15}$$

III. ANALYSIS OF THE FREE SPACE RADIATED FIELD

This Section highlights the main properties of the free space field radiated by an FDA, depending on its geometrical layout and on the frequency management policy. In agreement with previous studies ([1], [3], [5], [10], [11], [12] among others), the investigation is limited to the spatial

TABLE 2. Array Factor simulation parameters.

Parameter	Value
f_0	3.5 GHz
Δf	10 MHz
(M, N)	(5,1), (5,5) or (25,1)
Linear spacing	$\lambda_0/2$
Distance range	10 m – 100 m
Angle range	$-90°$ - $90°$
P_t	R_t = 50m, $\theta_t = 0°$

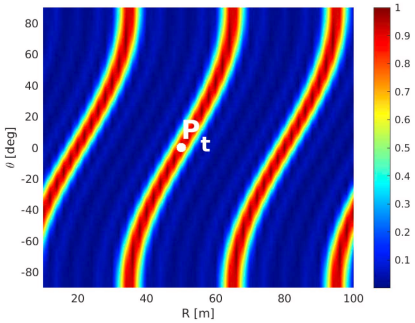

FIGURE 4. Normalized $|AF|^2$ for a linear FDA with M = 5 and linear frequency increase.

and temporal properties of $|AF(P,t)|^2$, i.e., omnidirectional radiation pattern in the (R,θ) plane is assumed for the array elements. The array factors have been computed and compared for the different FDA layouts according to eq. (4), eq. (11) and eq. (14). The size of the considered service area, the position of the target point as well as the main parameter of the FDA are summarized in Table 2. The analysis is carried out in both the spatial and the temporal domain.

A. SPATIAL DOMAIN

Fig. 4 shows the typical, S-shaped spatial representation of $|AF|^2$ for a linear FDA with linear frequency increase. The array factor clearly peaks in P_t but also quite elsewhere, and geofencing is therefore not effective for (safe) communication purposes. Although some improvement is brought by the logarithmic frequency offset (Fig. 5), the corresponding spotted area is still quite large and somehow misshapen. Increasing the number of elements brings clear further benefit overall (Fig. 6), but also makes the focus area even more awkwardly stretched. Spreading the M frequencies among the array elements in a random-like fashion can also improve the geofencing effect, as previously discussed in [22] for the logarithmic frequency offset and here shown in Fig. 7 when a linear frequency increment is instead considered. To the best of the authors' knowledge, this solution has never been investigated in previous studies. It is worth pointing out that a random like distribution of the frequencies over the array can be achieved in many ways, with quite different outcomes case by case.

Arranging the same number of radiating elements on a single-ring circle looks like a better solution compared to the linear deployment, for both the linear (Fig. 8) and the

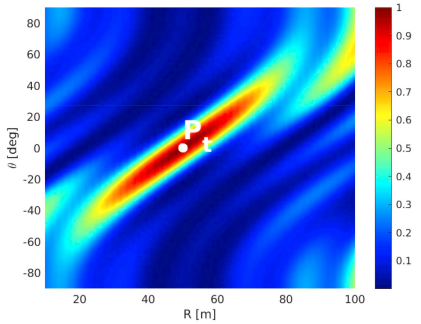

FIGURE 5. Normalized $|AF|^2$ for a linear FDA with M = 5 and logarithmic frequency increase.

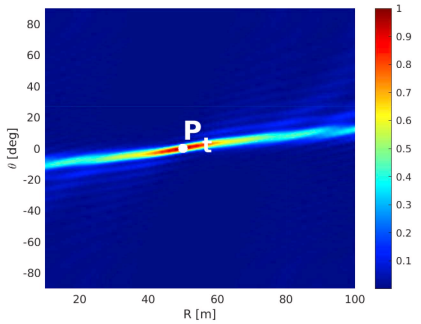

FIGURE 6. Normalized $|AF|^2$ for a linear FDA with M = 25 and logarithmic frequency increase.

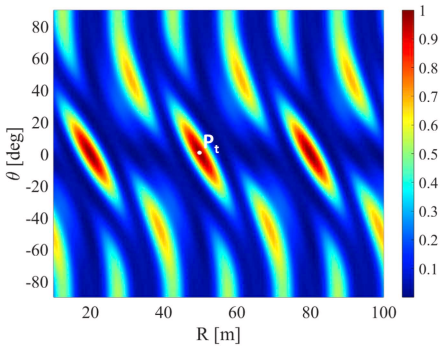

FIGURE 7. Normalized $|AF|^2$ for a linear FDA with M = 5 and linear frequency increase with random-like distribution.

logarithmic (Fig. 9) frequency increase. Surprisingly, the impact of the random-like distribution of the frequencies over the circular array (Fig. 10) turns out quite weaker than it has just been discussed for the linear deployment (Fig. 7). Based on this difference, which was also checked in some other cases not included here for the sake of the paper length, the random like frequency assignment will be limited in the following to the FDA linear deployment only.

A definitively sharper geofencing effect can be finally achieved if the FDA is constituted of many elements spread over a 2D spatial grid, as clearly reported in Fig. 11 and in Fig. 12 for the multi-ring circular layout and the planar layout, respectively.

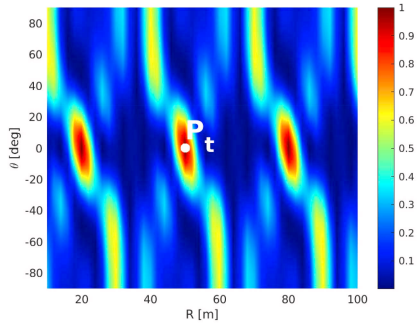

FIGURE 8. Normalized $|AF|^2$ for a circular FDA with M = 5, N = 1 and linear frequency increase.

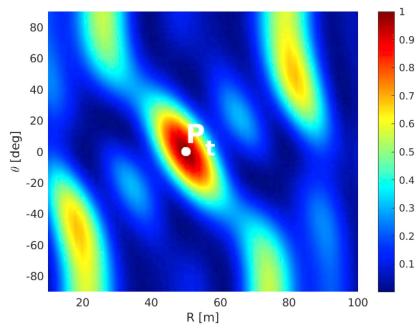

FIGURE 9. Normalized $|AF|^2$ for a circular FDA with M = 5, N = 1 and logarithmic frequency increase.

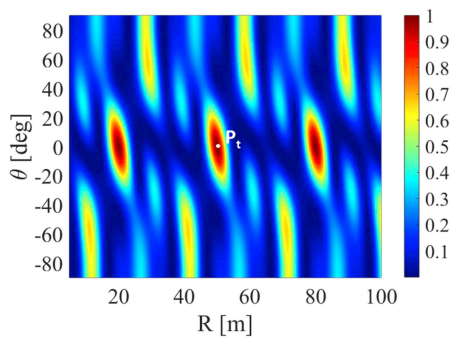

FIGURE 10. Normalized $|AF|^2$ for a circular FDA with M = 5, N = 1 and linear frequency increase with random like distribution.

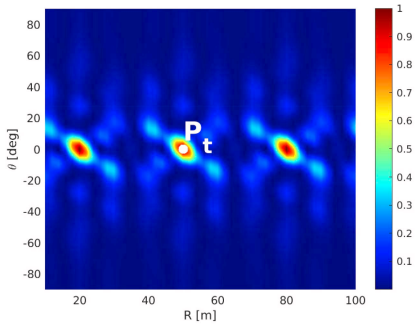

FIGURE 11. Normalized $|AF|^2$ for a circular FDA with M = 5, N = 5 and linear frequency increase.

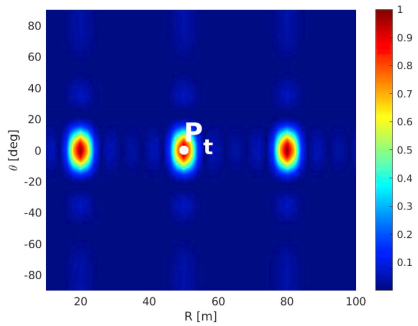

FIGURE 12. Normalized $|AF|^2$ for a planar FDA with M = 5, N = 5 and linear frequency increase.

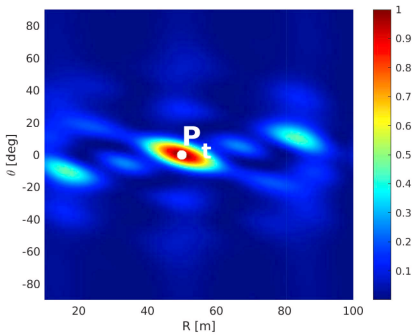

FIGURE 13. Normalized $|AF|^2$ for a circular FDA with M = 5, N = 5 and logarithmic frequency increase.

Results also highlight that the linear increase of frequency over the FDA elements trigger the spatial repetition of the array factor peaks in the radial direction, with spatial period equal to $c/\Delta f$ (Figs. 4, 7, 8, 10-12). The same effect does not rise up if the logarithmic frequency offset is instead enforced, as shown in Figs. 5, 6, 9, 13. Since the peak spatial repetition can in general result in a heavier interference/eavesdropping risk, the logarithmic frequency increase looks like the better solution. Nevertheless, it can turn out ineffective when it comes to the $|AF|$ properties in the time domain, as discussed in the following subsection. It is worth noting that the the spatial repetition of the spot due to the array factor periodicity is not automatically reflected in the field spatial distribution, as the intensity of the spots increasingly fades at larger distance because of path-loss. Therefore, multiple spots can actually reduce the FDA effectiveness to limit both the interference and the eavesdropping threat, especially in case the eavesdropper or the interfered user is placed on a beam spot closer to the transmitter than the target user. This occurrence can be limited if the spot spatial period is greater than the FDA - target point distance, i.e.:

$$R_t \leq \frac{c}{\Delta f} \tag{16}$$

B. TIME DOMAIN ANALYSIS

The time dependence of the array factor can represent an inherent advantage of FDA in radar applications, as it can provide automatic spatial scanning, but it requires

some care when it comes to wireless communications, or to any other service where the signal focusing should be conveniently steady in time. In fact, if the beam cannot stand still on the target point then (*i*) reliable exchange of information between two legitimate users could be possible over a limited time period only, and (*ii*) possible interference and/or eavesdropping may occur afterwards, as soon as the beam spot moves away. Of course these impairments can be overcome if the phases δ_m of the signals feeding the array elements can be reliably set at any time t according to the values required to keep the field spot on P_t. [1] Nevertheless, the required phase conditions are often enforced only at some specific instant t_0 for the sake of simplicity, as already discussed in Section II-A. Under such limitation, safe and reliable communications might still occur provided that the temporal behavior of the array factor turns out periodic, thus supplying the legitimate users with multiple time slots for reliable data exchange. This possibility is further discussed herein. In order that the legitimate users exploit the wireless channel only at the reappearance of the peak of the array factor, synchronization is of course required, but it represents an issue several wireless systems already cope with to an overall satisfactory extent. Furthermore, transmission might be interrupted as soon as the beam spot leaves the target point, thus preventing possible interference/leakages of information towards other users/eavesdropper placed around [19]. Still with reference to the list of parameters in Table 2, Fig. 14 shows the way $|AF|$ changes over time in the target point for a single ring circular array depending on the frequency increase policy. In the linear case, $|AF|$ is clearly periodic with period $T_{AF} = 1/\Delta f$, i.e., the peak value $|AF|_{max}$ turns up every T_{AF} sec.; conversely, the periodicity vanishes in the logarithmic case, and after t_0 $|AF|$ hardly rises up again to its maximum. Since data exchange between the users should take place only when signal geofencing is effectively enforced, i.e., when $|AF(P_t, t)| \approx |AF|_{max}$, the linear frequency increase looks like a more reliable solution. Moreover, it is worth noting that the logarithmic frequency increase also poses some technical problems, as the frequency increase becomes progressively smaller as the array size becomes larger. On the other hand, increasing the frequency linearly brings unpleasant periodicity in the spatial domain, as already pointed out in the previous subsection. More in general, peak periodicity in the space and in the time domain seem inherently interleaved: every time secure communication over long period between legitimate users is enabled through time periodicity of the array factor, spatial peak repetition turns up as an unavoidable side effect.

A greater number of elements over the ring of course increases the value of $|AF|$ at t_0, but also unexpectedly

[1] Anyway, it would not correspond to a static array factor. In fact, in spite of some alleged solutions for time invariant FDA have been proposed in some previous studies, the analysis carried out in [27] has definitively stated that a range-dependent pattern eventually always leads to a time-dependent pattern. Thus, it is impossible to generate a time-invariant range-dependent beam pattern.

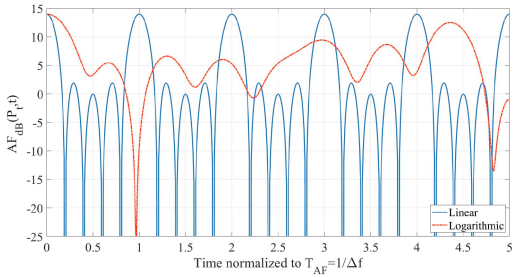

FIGURE 14. $|AF|$ vs. time in P_t for different policies of frequency increase across the elements of a single ring circular FDA.

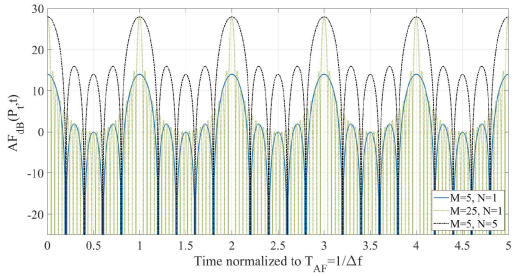

FIGURE 15. $|AF|$ vs. time in P_t for different number of rings and of elements per ring.

reduces the time $|AF|$ keeps closer to $|AF|_{max}$ (Fig. 15). For instance, the half-factor time-width, i.e., the time interval where $|AF|$ keeps greater than $|AF|_{max}/2$, drops from about 18% to 3.6% when M is increased from 5 to 25.

Interestingly, if the 25 elements are instead spread over 5 rings, corresponding to 5 different feeding frequencies instead of 25, the same increase in $|AF|_{max}$ is achieved while preserving the half-factor time-width at the same time (Fig. 15). This actually represents the main reason why the 2D layout (i.e., the circular and the planar ones) should be conveniently conceived with a number of different frequencies lower than the total number of array elements. Limiting the number of radiated frequencies can also contribute to reducing the overall FDA power consumption, as the generation and the management of the different frequencies might represent an energy demanding process inside the array front-end.

In summary, the space/time analysis carried out in previous Sections brings the following considerations:

- Effective FDA-based communications require the beam spot reliably placed on the target point for a time much longer than the symbol length;
- In case the phase conditions to keep the field peak on the target point can be tuned over time, then a logarithmic frequency increase can be considered, to get rid of the peak spatial repetition;
- By contrast, if the required phase settings are instead enforced at some specific instant t_0 only, then the linear frequency increase appear as the viable solution, as it provides periodic time slots for data exchange. The efficiency of the communication can be improved by

spreading the array elements over a 2D spatial grid and by considering numerous radiating elements, with a number of different frequencies conveniently lower than the array size.

- The periodicity in time of the array factor always comes together with periodicity in the range domain, which can be potentially harmful.

IV. GEOFENCING SENSITIVITY TO ARRAY PARAMETERS

The sensitivity of the geofencing effect to the FDA parameters is here investigated by means of two specific parameters, namely the *focus area* (A_f) and the *focus efficiency* (ε_f). The focus area is defined as the area around the target point P_t where the normalized $|AF|^2_{dB}$ is greater than -3dB, whereas the focus efficiency is computed as:

$$\varepsilon_f = \frac{A_f}{\sum_{s=1}^{N_s} A_s \cdot \left(\frac{R_t}{R_s}\right)^2} \tag{17}$$

being R_t the distance of the target point from the transmitting FDA, N_s the number of spots over the service area where $|AF|^2_{dB}$ is greater than -3 dB, A_s the area of the s-th spot and R_s its distance from the FDA. The focus area of course accounts for the geofencing effectiveness on the target point, whereas the focus efficiency accounts for the presence of multiple spots over the service area. Although ideal geofencing of course corresponds to ε_f equal to 1, an efficiency greater than 0.5 may represent an acceptable target, meaning that the spurious spots are overall smaller than the target spot or - otherwise - that they are further from the transmitting FDA than the target point, and therefore exposed to heavier attenuation. With reference to A_f, it should not exceed some tens of square meters as a fair rule of thumb.

In particular, the spatial average of the focus area and efficiency ($\langle A_f \rangle$ and $\langle \varepsilon_f \rangle$, respectively) is computed herein for different characteristics of the FDA. The statistical assessment is carried out through a Monte Carlo approach. For each considered setting of the FDA (geometrical layout, number of elements and spacing, frequency offset), A_f and ε_f have been computed for $N_t = 1000$ target points uniformly spread over the service area, and the N_t corresponding values have been finally averaged to get the spatial means. The investigation is limited to the linear frequency increase across the elements, which is expected to be more critical in terms of focus efficiency because of the peak spatial repetition. The circular layout is first addressed as a reference deployment, and it is then compared to the planar and the linear solutions. Random-like distribution of the frequencies among the radiating elements is considered in the linear case, as it has been found especially striking just for the linear deployment (see Section III-A)

To begin with, the same service area considered in Table 2 ($10m \leq R \leq 100m, -90^o \leq \theta \leq 90^o$) has been also considered, and the spacing between the elements has been set equal to $\lambda_0/2$.

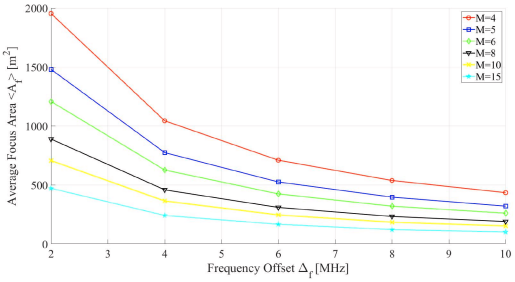

FIGURE 16. Average focus area, single ring circular FDA, R ≤ 100m, f_0 = 3.5GHz, spacing = $\lambda_0/2$.

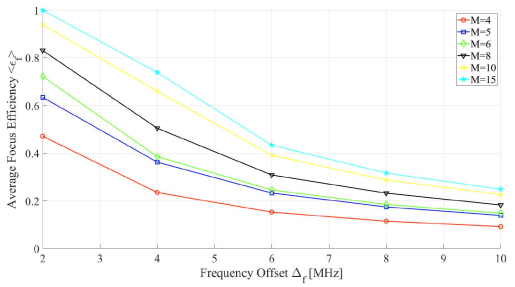

FIGURE 17. Average focus efficiency, single ring circular FDA, R ≤ 100m, f_0 = 3.5GHz, spacing = $\lambda_0/2$.

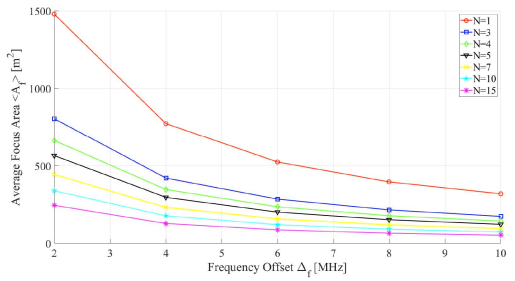

FIGURE 18. Average focus area, multiple rings circular FDA, M = 5, R ≤ 100m, f_0 = 3.5GHz, spacing = $\lambda_0/2$.

A. CIRCULAR DEPLOYMENT

The average focus area and efficiency for a single ring circular array are plotted in Figs. 16 and 17 against Δf and for different M values. Increasing the frequency offset leads to smaller focus area but unfortunately also to lower efficiency, as the spots' radial period gets shorter, and therefore eq. (16) results unsatisfied over an increasingly larger part of the service area. This increases the occurrence of cases where additional spots closer to the transmitting FDA turn up, to the detriment of the mean focus efficiency. A greater number of radiating elements over the ring turns out beneficial on both $\langle A_f \rangle$ and $\langle \varepsilon_f \rangle$, although it makes harder to meet the condition stated in eq. (7). Moreover, the benefit reduces as M increases, especially for the focus efficiency. A large number of elements also impairs the sensitivity of the focus area to the frequency offset (Fig. 16).

The introduction of multiple rings can further improve both the focus area and efficiency (Figs. 18 and 19),

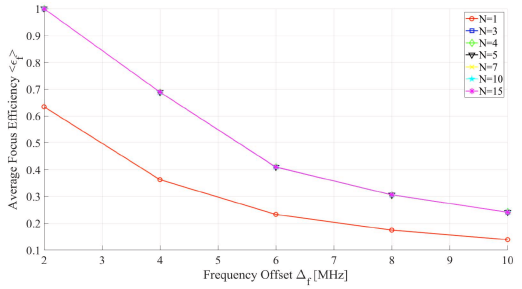

FIGURE 19. Average focus efficiency, multiple rings circular FDA, M = 5, R ≤ 100m, f_0 = 3.5GHz, spacing = $\lambda_0/2$.

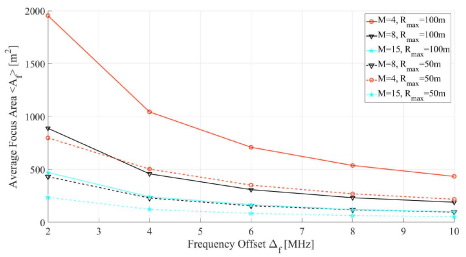

FIGURE 20. Impact of range restriction on the focus area for a single ring circular FDA, f_0 = 3.5GHz, spacing = $\lambda_0/2$.

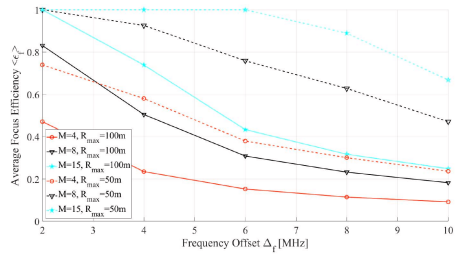

FIGURE 21. Impact of range restriction on the focus efficiency for a single ring circular FDA, f_0 = 3.5GHz, spacing = $\lambda_0/2$.

although $\langle \varepsilon_f \rangle$ turns out to be insensitive to the number of rings.

These results clearly show that Δf should be limited to few MHz to get a satisfactory efficiency, but this contrasts with the requirement empirically set on the focus area. In fact, according to Figs. 16 and 18, even numerous rings and/or elements over each ring can hardly provide $\langle A_f \rangle$ smaller than some hundreds of square meters for Δf up to few MHz.

Performance can be improved by limiting the extension of the service area, i.e., the maximum distance where the geofencing effect is enforced. Figs. 20 and 21 compare the average focus area and efficiency in case the maximum range is set to 100m and 50m. Of course, the range reduction automatically makes eq. (16) more easily satisfied, thus corresponding to higher efficiency (Fig. 21). Moreover, figures like Figs. 11 and 12 show that radial spots keep their shape in the *polar* plane, i.e., their area grows up with distance. Therefore, limiting the range is also beneficial to $\langle A_f \rangle$ (Fig. 20).

The impact of the communication frequency and of the spacing between the array elements on the geofencing effectiveness is finally reported in Figs. 22 and 23.

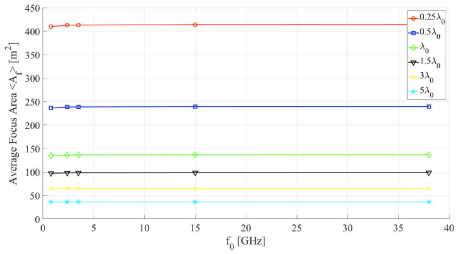

FIGURE 22. Focus area sensitivity to communication frequency and elements spacing for a circular FDA with M = 5, N = 5, Δ_f = 5*MHz*.

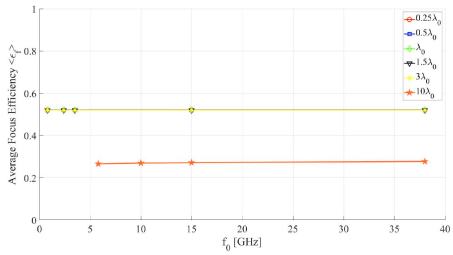

FIGURE 23. Focus efficiency sensitivity to communication frequency and elements spacing for a circular FDA with M = 5, N = 5, Δ_f = 5*MHz*.

Both $\langle A_f \rangle$ and $\langle \varepsilon_f \rangle$ seem independent of the frequency, whereas increasing the spacing reduces the focus area while keeping the efficiency basically unchanged, unless it is excessively stretched (Fig. 23). In fact, as a large spacing can boost the side lobes level in standard arrays, it can similarly trigger the appearance of "side spots" in the angular direction, to the disadvantage of the focus efficiency.

In conclusion, many parameters seem to affect the focus area, like the frequency offset, the number of elements and their spacing, whereas the focus efficiency is mainly driven by the frequency offset. Therefore, it can be convenient to choose M, N and the spacing to get a satisfactory (average) focus area, and select Δf in order to meet also the requirement on the (average) focus efficiency. In this general framework, it is worth reminding that limiting the range also turns out to be beneficial, i.e., signal geofencing through FDA seems a viable solution only for short- / mid-range wireless communications, as also previously suggested by eq. (16). For instance, setting the maximum range at 50m, M=N=5, Δf = 4MHz and with spacing equal to $3\lambda_0$, then $\langle A_f \rangle \approx 32m^2$ and $\langle \varepsilon_f \rangle = 1$.

B. COMPARISON WITH PLANAR AND LINEAR DEPLOYMENT

As shown in Figs. 24 and 25, the performance achieved for the linear and planar layouts follows the same trends already highlighted for the circular case.

For the same array parameters, a planar FDA in general exhibits worse performance than the corresponding circular FDA in terms of both focus area and efficiency. Conversely, a linear FDA (with random-like frequency spreading) can yield a quite limited focus area, in general well smaller compared to a circular or planar array with the same number

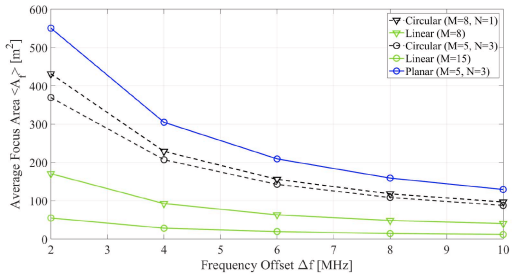

FIGURE 24. Average focus area in the linear and in the planar case, comparison with the circular layout. $f_0 = 3.5$ GHz, spacing $= \lambda_0/2$, $R_{max} = 50$m

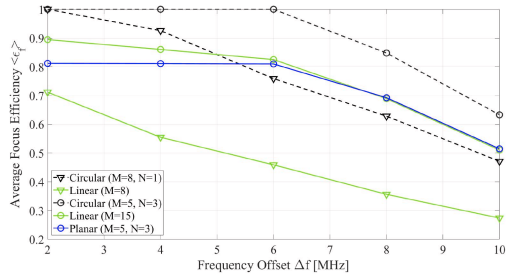

FIGURE 25. Average focus efficiency in the linear and in the planar case, in comparison with the circular layout. $f_0 = 3.5$ GHz, spacing $= \lambda_0/2$, $R_{max} = 50$m.

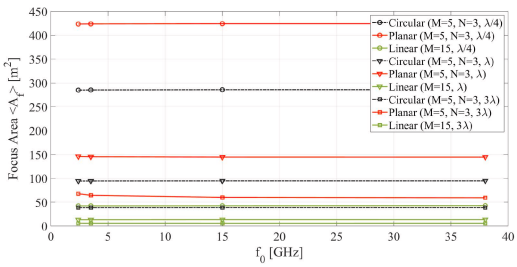

FIGURE 26. Average focus area in the linear and in the planar case, comparison with the circular layout. $\Delta f = 5$ MHz, $R_{max} = 50$m.

of elements (Fig. 24). Unfortunately, the linear deployment turns out to be less efficient than the circular layout with the same number of transmitting antennas (Fig. 25). It is worth pointing out that the random-like distribution of frequencies over the array can be done in different ways, corresponding to different realizations of $|AF|$ in the (R, θ) plane. This property can be exploited to make geofencing more effective. In fact, enforcing a random-like time swap of the frequencies across the array elements may result in a correspondingly frantic change of the spurious spots position around the target spot. This effect can further hamper any possible eavesdropping attack, as well as fairly share interference all over the space rather than keep it affecting few specific locations (in a sort of *interference hopping* effect).

In comparison with the circular deployment, a larger spacing between the elements is less effective in both the linear and the planar case, as it still reduces the size of the focus area (Fig. 26) but it also affects the focus efficiency to a heavier extent (Fig. 27).

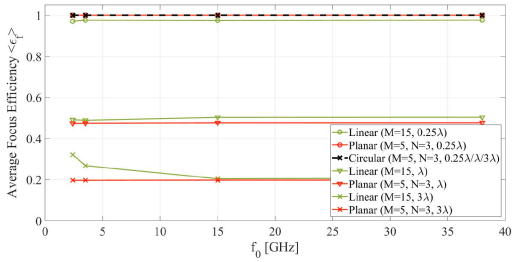

FIGURE 27. Average focus efficiency in the linear and in the planar case, in comparison with the circular layout. $\Delta f = 5$ MHz, $R_{max} = 50$m.

The major trends and results highlighted by the analysis carried out in Section IV are summed up in Table 3, which reports the sensitivity of the focus area and efficiency to the main parameters of the FDA.

V. A GLANCE TO MULTIPATH EFFECT

In agreement with several previous studies [1], [5], [6], [9], propagation in ideal free space conditions has been considered so far. Nevertheless, FDAs might be also deployed in complex environments, where shadowing and/or multipath effects may rise up. The impact of multipath on FDA performance is here preliminary addressed in the simple case sketched in Fig. 28, where the presence of a Perfect Electrical Conductor (PEC) reflecting surface introduces a reflected propagation path in addition to the direct contribution [28]. Compared to [29], where the main focus was not on propagation issues and the ground effect was taken into account through a random fading coefficient, a deterministic approach is here considered, which can more easily highlight the way multipath can affect geofencing effectiveness. The final, analytical formulation achieved herein is actually rougher than the field expressions proposed in [28], but it is also clearly simpler and more reader-friendly, and therefore more suited to straightforwardly convey the message that multipath effects should be taken into account when FDAs are deployed in real propagation scenarios.

Under the assumption $R >> h_{FDA}, h_{P_t}$ (Fig. 28), the total field received at frequency f_m (E^m_{tot}) can be formally expressed through a correction factor simply applied to the free space field (E^m_{fs}) [30], i.e.:

$$E^m_{tot} = E^m_{FS} \cdot CF_m = E^m_{FS} \cdot \left(1 + \Gamma_m \cdot e^{-j\beta_m \Delta r}\right) \qquad (18)$$

where CF_m is the correction factor, Γ_m and β_m are the reflection coefficient and the wave number at frequency f_m, respectively, and $\Delta r \approx 2h_{FDA} \cdot h_{P_t}/R$. Since the reflecting surface is made of PEC, $\Gamma_m = -1$, $\forall m$. Let's also assume for the sake of simplicity that Δf_m is so smaller than f_0 (eq. (7)) that $\beta_m \approx \beta_0$ in eq. (18). Then:

$$E^m_{tot} \approx E^m_{FS} \cdot CF_0 = E^m_{FS} \cdot \left(1 - e^{-j\beta_0 \Delta r}\right) \qquad (19)$$

Under the considered assumptions the signals received at different frequencies in presence of the ground approximately add up as they do in free space, i.e., the FDA array factor

TABLE 3. Sensitivity of focus area and efficiency to the major array parameters.

	↑ Δf	↑M	↑N	↑ f_0	↑Spacing	↑Range
Focus Area	↓	↓	↓	–	↓	↑
Focus Efficiency	↓	↑	– (approx.)	–	– (circular) ↓ (planar/linear)	↓

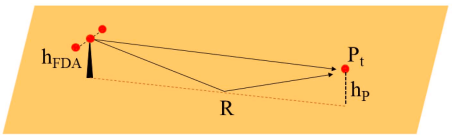

FIGURE 28. FDA propagation in presence of a PEC reflecting surface.

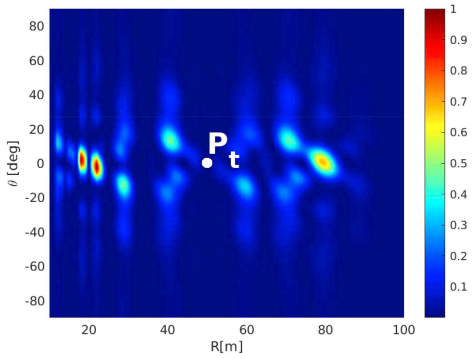

FIGURE 29. Possible effect of a PEC reflecting surface on propagation from a circular FDA with $M = N = 5$, $f_0 = 3.5$ GHz, $\Delta f = 10$ MHz, target point $P_t(50m, 0°)$ and $h_{FDA} = 3$ m, $h_P = 1$ m.

can be still leveraged to express the total received free space field, i.e.:

$$|E_{tot}(P,t)| \approx |E_0(P)| \cdot |AF(P,t)| \cdot |CF_0(P)| \tag{20}$$

According to [30], the magnitude of the correction factor can be expressed as:

$$|CF_0| = \left[2 \left| \sin\left(\frac{2\pi}{\lambda_0} \frac{h_{FDA} \cdot h_P}{R} \right) \right| \right] \tag{21}$$

At large distance, where $sin(\frac{1}{R}) \approx \frac{1}{R}$, the interference between the direct and the reflected waves keeps steadily destructive, and the received signal intensity decreases over distance at a rate harsher than free space. At shorter distances, the presence of the PEC reflecting surface introduces fluctuations on the received signal strength in both the frequency and the range domains, depending on whether the interference is constructive or destructive. In case it turns out destructive in P_t, the total received field can be dramatically weak regardless of the array factor. This is clearly highlighted in Fig. 29, where the same situation already considered in Fig. 11 under free space conditions is reconsidered taking into account the PEC reflecting surface effect by means of the approximated eq. (20).

To what extent FDA-based wireless application can cope with multipath propagation looks like a critical issue, which requires more accurate and specific attentions. In this respect, FDA performance and focus effectiveness in multipath and NLoS scenarios has been also preliminarily investigated in [31] through ray tracing simulations, highlighting that multipath can introduce additional small-scale spatial oscillations on the array factor.

VI. MULTI-USERS FDA COMMUNICATIONS

In the previous sections, possible benefits coming from FDA to interference control or communication secrecy have been investigated with reference to a single wireless transmitter spreading the FDA signal over a service area. Nevertheless, many users can be simultaneously active in real wireless networks, and therefore some general considerations on multi-users FDA communications are shortly drawn in this section.

A first, possible solution to enable FDA in multi-users scenarios may be represented by time division multiple access (TDMA), where the different FDA transmissions are arranged on different time slots. In order that TDMA can effectively work, it should carefully take into account the time instability of the array factor, i.e., the time slot handling policy should enable each communication when the corresponding beam spot is well-placed on the target receiver. Simple management of multiple transmissions at the base station (BS)/access point (AP) might be also achieved by splitting the whole array into sub-arrays then assigned to the different communications, to the expense of the final geofencing effectiveness resulting from the reduction in the number of antenna elements allocated to each user. In case a heavier level of complexity can be afforded, downlink FDA transmissions toward different users can even exploit the whole array by means of multiple, simultaneous beams enforced by means of different beamforming matrixes [32].

Finally, FDA technique looks quite consistent with Orthogonal Frequency Division Multiplexing (OFDM) modulation and access, which is currently widely employed in many wireless communication systems. In OFDM the symbols sequence is split into several, parallel streams, which are then transmitted on different frequencies (sub-carriers). Therefore, mapping the same symbol on the different sub-carriers should in the end correspond to FDA. In order to get a suitable frequency offset, just a sub-set of the available sub-carriers should be probably used, but a flexible, dynamic exploitation of the sub-carriers does not represent an issue for the current state of OFDM technology. More in general, FDA design can be expected to share the same hardware complexity and challenges of (MIMO-)OFDM transceiver [33]. Further details on OFDM technology to

enable FDA-based secure wireless communications can be found in [34], whereas in [35] the FDA technique is embedded in an OFDM modulation scheme for joint communication and sensing.

VII. CONCLUSION

Frequency diverse arrays exploit feeding signals with different frequency and phase to achieve signal geofencing, i.e., to focus the radiated field around some target point. Although commonly envisaged for radar and wireless power transfer applications, frequency diverse arrays can be in principle helpful also in wireless communications, to limit the interference issue and/or to improve data privacy. In order to understand whether these benefits can be really achieved in practice, investigating the sensitivity of the geofencing effect to the main parameters of the array is an important task, which has been addressed in this work. As general remarks, FDA based communications can cope with users' mobility to a limited extent, i.e., they look more suited to static communication systems. Frequencies can increase over the array according to either a logarithmic or a linear policy. In case geofencing can't be enforced all over the time by tuning the phase of the array feeding signals accordingly, the linear frequency increase should be considered, as it can at least provide the transmitter and the receiver with multiple, periodic communication time slots. A random-like distribution of the frequencies across the elements can be effective, although the benefit basically holds for the array linear deployment much more than for other geometrical layouts. The frequency offset should not exceed a few MHz, to get a satisfactory focus efficiency, and also to keep frequency deviations usefully small. In order to improve the performance, employing numerous elements is also convenient, better if spread on a two-dimensional grid (e.g., circular or planar) and grouped in clusters sharing the same feeding frequency. Increasing the spacing between the elements can also reduce the focus area, of course at the expense of the array size, but can also impair the focus efficiency on the other hand, at least for the linear and the planar layouts. Overall, pursuing satisfactory focus area and efficiency looks like a complex trade-off, that can be relieved if geofencing is limited to mid- / short-range communications.

Further investigations are necessary to assess the performance of frequency diverse arrays in presence of multipath, which has been here proved to represent a possible threat just in a simple reference case. Moreover, evaluation of the geofencing effectiveness in case the FDA is made by directive radiating elements also deserves additional, specific attention.

APPENDIX

A. LINEAR DEPLOYMENT

With reference to the linear FDA previously outlined in Fig. 1, the free space field radiated by the m-th element in $P(R,\theta)$ at time instant t can be written as:

$$e_m(R,\theta,t) = \Re\left\{\left(\frac{E_{0m}}{R_m}e^{j\delta_m}e^{-j\beta_m R_m}\right)e^{j2\pi f_m t}\right\} \tag{A.1}$$

where E_{0m} is the complex field emitted in the θ direction, $\beta_m = 2\pi/\lambda_m$ and R_m the distance traveled by the m-th signal. In far field conditions, the signals arriving in P from each array element basically experience the same path-loss, i.e.,:

$$1/R_m \approx 1/R \tag{A.2}$$

Conversely, the following expression for R_m should be considered in the exponential to account for the phase shift due to propagation (Fig. 1):

$$R_m \approx R - md\sin\theta \tag{A.3}$$

being d the spacing between the elements (Fig. 1). Furthermore,

$$\frac{1}{\lambda_m} = \frac{f_m}{c} = \frac{f_0}{c} + \frac{\Delta f_m}{c} \tag{A.4}$$

$$e_m(R,\theta,t) = \Re\left\{\left(\frac{E_{0m}}{R}e^{j\delta_m}e^{-j\overbrace{\frac{2\pi f_0}{c}}^{\beta_0}R}e^{j\frac{2\pi m f_0 d\sin\theta}{c}}e^{-j\frac{2\pi\Delta f_m(R-md\sin\theta)}{c}}e^{j2\pi\Delta f_m t}\right)e^{j2\pi f_0 t}\right\}$$
$$= \Re\left\{\left(\frac{E_{0m}}{R}e^{-j\beta_0 R}\right)\left(e^{j\delta_m}e^{j\frac{2\pi m f_0 d\sin\theta}{c}}e^{-j\frac{2\pi\Delta f_m(R-md\sin\theta)}{c}}e^{j2\pi\Delta f_m t}\right)e^{j2\pi f_0 t}\right\} \tag{A.6}$$

$$e(R,\theta,t) = \sum_{m=0}^{M-1}\Re\left\{\left(\frac{E_0}{R}e^{-j\beta_0 R}\right)\left(e^{j\delta_m}e^{j\frac{2\pi f_0 md\sin\theta}{c}}e^{-j\frac{2\pi\Delta f_m(R-md\sin\theta)}{c}}e^{j2\pi\Delta f_m t}\right)e^{j2\pi f_0 t}\right\}$$
$$= \Re\left\{\underbrace{\left(\frac{E_0}{R}e^{-j\beta_0 R}\right)}_{E_0(P)}\left[\underbrace{\sum_{m=0}^{M-1}e^{j\delta_m}e^{j\frac{2\pi f_0 md\sin\theta}{c}}e^{-j\frac{2\pi\Delta f_m(R-md\sin\theta)}{c}}e^{j2\pi\Delta f_m t}}_{AF(P,t)}\right]e^{j2\pi f_0 t}\right\} \tag{A.7}$$

and the field $e_m(R, \theta, t)$ can be then expressed as in eq. (A.6).

Finally, the total field radiated by the FDA in P at time t can be computed as the sum of the fields from each element. In case $E_{0m} \approx E_0$ can be also assumed, the final expression reported in eq. (A.7) can be achieved, where the total, complex field $e(P, t)$ therefore corresponds to the product of the complex field radiated by the single, reference element ($E_0(P)$ in eq. (A.7)) and a complex array factor $AF(P, t)$ equal to:

$$AF(R, \theta, t) = \sum_{m=0}^{M-1} e^{j\delta_m} e^{j\frac{2\pi f_0 md \sin\theta}{c}} e^{-j\frac{2\pi \Delta f_m (R - md\sin\theta)}{c}} e^{j2\pi \Delta f_m t} \quad \text{(A.5)}$$

REFERENCES

[1] W.-Q. Wang, H. C. So, and A. Farina, "An overview on time/frequency modulated array processing," *IEEE J. Sel. Topics Signal Process.*, vol. 11, no. 2, pp. 228–246, Mar. 2017.

[2] P. Antonik and M. C. Wicks, "Frequency diverse array radars," in *Proc. IEEE Radar Conf.*, 2006, pp. 215–217.

[3] W.-Q. Wang, "Frequency diverse array antenna: New opportunities," *IEEE Antennas Propag. Mag.*, vol. 57, no. 2, pp. 145–152, Apr. 2015.

[4] S. Ke, M. He, X. Bu, and W. Cai, "A leakage-based directional modulation scheme for frequency diverse array in robot swarm networks," *IEEE Access*, vol. 8, pp. 107823–107837, 2020.

[5] W. Khan, M. Qureshi, and S. Saeed, "Frequency diverse array radar with logarithmically increasing frequency offset," *IEEE Antennas Wireless Propag. Lett.*, vol. 8, pp. 499–502, 2015.

[6] J. Xu, G. Liao, S. Zhu, L. Huang, and H. So, "Joint range and angle estimation using MIMO radar with frequency diverse array," *IEEE Trans. Signal Process.*, vol. 63, no. 13, pp. 3396–3410, Jul. 2015.

[7] W.-Q. Wang, "Overview of frequency diverse array in radar and navigation applications," *IET Radar, Sonar Navig.*, vol. 10, no. 6, pp. 1001–1012, 2016.

[8] C. Sammartino, C. J. Baker, and H. D. Griffiths, "Frequency diverse MIMO techniques for radar," *IEEE Trans. Aerosp. Electron. Syst.*, vol. 49, no. 1, pp. 201–222, Jan. 2013.

[9] E. Fazzini, A. Costanzo, and D. Masotti, "Ad-hoc WPT exploiting multi-sine excitation of linear frequency diverse arrays," in *Proc. Wireless Power Week*, 2022, pp. 563–566.

[10] E. Fazzini, M. Shanawani, A. Costanzo, and D. Masotti, "A logarithmic frequency-diverse array system for precise wireless power transfer," in *Proc. 50th Eur. Microw. Conf. (EuMC)*, 2021, pp. 646–649.

[11] S. Y. Nusenu, "Development of frequency modulated array antennas for millimeter-wave communications," *Wireless Commun. Mobile Comput.*, vol. 2019, pp. 1–15, Apr. 2019.

[12] S. Y. Nusenu and A. Basit, "Frequency diverse array antennas: From their origin to their application in wireless communication systems," *J. Comput. Netw. Commun.*, vol. 2018, pp. 1–12, May 2018.

[13] J. Xiong, Y. N. Shaddrack, and W. Wen-Qin, "Directional modulation using frequency diverse array for secure communications," *Wireless Pers. Commun.*, vol. 95, pp. 2679–2689, Jan. 2017.

[14] J. M. Hamamreh, H. M. Furqan, and H. Arslan, "Classifications and applications of physical layer security techniques for confidentiality: A comprehensive survey," *IEEE Commun. Surveys Tuts.*, vol. 21, no. 2, pp. 1773–1828, Sep. 2019.

[15] J. M. Lin, Q. M. Li, J. Yang, H. Shao, and W.-Q. Wand, "Physical-layer security for proximal legitimate user and eavesdropper: A frequency diverse array beamforming approach," *IEEE Trans. Inf. Forensics Security*, vol. 13, pp. 671–684, 2018.

[16] A. Nessa, B. Adhikari, F. Hussain, and X. Fernando, "A survey of machine learning for indoor positioning," *IEEE Access*, pp. 214945–214965, 2020.

[17] P. Meissner and K. Witrisal, "Multipath-assisted single-anchor indoor localization in an office environment," in *Proc. 19th Int. Conf. Syst., Signals Image Process. (IWSSIP)*, 2012, pp. 22–25.

[18] J. Xiong, W.-Q. Wang, H. Shao, and H. Chen, "Frequency diverse array transmit beampattern optimization with genetic algorithm," *IEEE Wireless Antennas Wireless Propag. Lett.*, vol. 16, pp. 469–472, 2017.

[19] E. Fazzini, A. Costanzo, and D. Masotti, "Range selective power focusing with time-controlled bi-dimensional frequency diverse array," in *Proc. IEEE Wireless Power Trnsfer Conf.*, 2021, pp. 1–4.

[20] Y. Hong, X. Jing, H. Gao, and Y. He, "Fixed region beamforming using frequency diverse subarray for secure mmWave wireless communications," *IEEE Trans. Inf. Forensics Security*, vol. 15, pp. 2706–2721, 2020.

[21] W.-Q. Wang, "Range-angle dependent transmit beampattern synthesis for linear frequency diverse arrays," *IEEE Trans. Antennas Propag.*, vol. 61, no. 8, pp. 4073–4081, Aug. 2013.

[22] G. Huang, Y. Ding, S. Ouyang, and V. Fusco, "Frequency diverse array with random logarithmically increasing frequency offset," *Microw. Opt. Technol. Lett.*, vol. 62, no. 7, pp. 2554–2561 , 2020.

[23] X. Wu, H. Shao, J. Lin, Q. Li, and Q. Shi, "High-speed user-centric beampattern synthesis via frequency diverse array," *IEEE Trans. Signal Process.*, vol. 69, pp. 1226–1241, 2021.

[24] S. Goel and R. Negi, "Guaranteeing secrecy using artificial noise," *IEEE Trans. Wireless Commun.*, vol. 7, no. 6, pp. 2180–2189, Jun. 2008.

[25] S. Ji, W. Wang, H. Chen, and Z. Zheng, "Secrecy capacity analysis of AN-aided FDA communication over Nakagami-m fading channels," *IEEE Wireless Commun. Lett.*, vol. 7, no. 6, pp. 1034–1037, Dec. 2018.

[26] E. Fazzini, A. B. Gok, A. Costanzo, and D. Masotti, "Accurate ranging exploiting a 32-patch frequency diverse array with circular symmetry," in *Proc. 16th Eur. Conf. Antennas Propag. (EuCAP)*, 2022, pp. 1–5.

[27] K. Chen, S. Yang, Y. Chen, and S.-W. Qu, "Accurate models of time-invariant beampatterns for frequency diverse arrays," *IEEE Trans. Antennas Propag.*, vol. 67, no. 5, pp. 3022–3029, May 2019.

[28] C. Centipete and S. Demir, "Multipath characteristics of frequency diverse arrays over a ground plane," *IEEE Trans. Antennas Propag.*, vol. 62, no. 7, pp. 3567–3574, Jul. 2014.

[29] Q. Cheng, S. Wang, V. Fusco, F. Wang, J. Zhu, and C. Gu, "Physical-layer security for frequency diverse array-based directional modulation in fluctuating two-ray fading channels," *IEEE Trans. Wireless Commun.*, vol. 20, no. 7, pp. 4190–4204, Jul. 2021.

[30] J. Parsons, *Fundamentals of VHF and UHF Propagation*. Hoboken, NJ, USA: Wiley, ch. 2, pp. 15–31. [Online]. Available: https://onlinelibrary.wiley.com/doi/abs/10.1002/0470841524.ch2

[31] S. Del Prete, F. Fuschini, M. Barbiroli, and M. Zadeh, "A study on propagation of frequency diverse array in multipath environments," in *Proc. IEEE-APS Topical Conf. Antennas Propag. Wireless Commun. (APWC)*, 2023, pp. 90–94.

[32] J. Jian, W. Wang, H. Chen, and B. Huang, "Physical-layer security for multi-user communications with frequency diverse array-based directional modulation," *IEEE Trans. Veh. Technol.*, vol. 27, no. 8, pp. 10133–10145, Aug. 2023.

[33] C. D. Murphy, "Low-complexity FFT structures for OFDM transceivers," *IEEE Trans. Commun.*, vol. 50, no. 12, pp. 1878–1881, Dec. 2002.

[34] Y. Ding, J. Zhang, and V. Fusco, "Frequency diverse array OFDM transmitter for secure wireless communication," *Electron. Lett.*, vol. 51, no. 17, pp. 1374–1376, 2015.

[35] H. Huang and W.-Q. Wang, "FDA-OFDM for integrated navigation, sensing, and communication systems," *IEEE Aerosp. Electron. Syst. Mag.*, vol. 33, nos. 5–6, pp. 34–42, May/Jun. 2018.

Open Access funding provided by 'Alma Mater Studiorum - Università di Bologna' within the CRUI CARE Agreement